Machine-learned material indices: Final Report

Patrick Walgren and Roshan Suresh Kumar
Department of Aerospace Engineering
Texas A&M University
College Station, TX 77845

Abstract

The process of materials selection involves determining a hyperplane in the space of material and/or geometric properties that contains the optimal set of materials and selecting candidate materials based on additional requirements. This hyperplane is represented by a performance metric and is parameterized by performance indices, which quantify the relative influence of the material and geometric properties on this hyperplane. In traditional materials selection, the visualization methods developed by Ashby are widely used. These methods work for simple problems but more complex problems involving nonlinear mapping between multiple material and geometric features and the performance index to be optimized require a more generalized approach. This project attempts to determine the performance metric for thermomechanical hot shock problem considering two dissimilar materials using machine-learning based feature selection. The concept is first tested on a beam bending problem and then applied to the hot shock problem.

1 Introduction

Selection of materials for an application is an important aspect of product design. The goal of this process is to down select from a set of candidate materials based on the impact of material properties on the performance of the resulting design. Traditionally, materials selection involves visual analysis of the various materials in the material and geometric properties space and analytical solutions for the dominant physics to identify an invariant performance metric shared by the most optimal materials [1]. Example material indices include σ_y/ρ for light and strong ties, σ_f^2/E for small springs, and $a^{1/2}/\lambda$ for energy-efficient kiln walls[1]. More example structural material indices are shown in figure 1. As the complexity of problems increases, identification of the performance metric through visual and analytical means becomes increasingly difficult, to the point where discerning combinations of different material and geometric properties to create the invariant hyperplane is nearly impossible. To address this issue, this project attempts to use machine learning-based feature selection to determine the most compact set of material and geometric properties that can constitute the invariant performance metric hyperplane. The optimal set of materials and/or geometries is then determined by optimizing a certain material property and subsequently used to find performance indices corresponding to the selected features using a separate optimization routine.

Lu and Fleck investigated thermal shock for a single infinite homogeneous plate and came up with the performance metrics for the problem [2]. This project extends the analysis to a hot shock problem with different materials bonded together. As is explained in Section 4, this problem is more complicated due to interface interactions and the additional influence of geometry. Two approaches for this problem are proposed: an unsupervised feature selection based optimization and a neural network

[1] In these examples, σ_y and σ_f denote the material yield and failure stress, respectively; ρ and E describe the material density and Young's modulus; and a and λ are the material thermal diffusivity and conductivity.

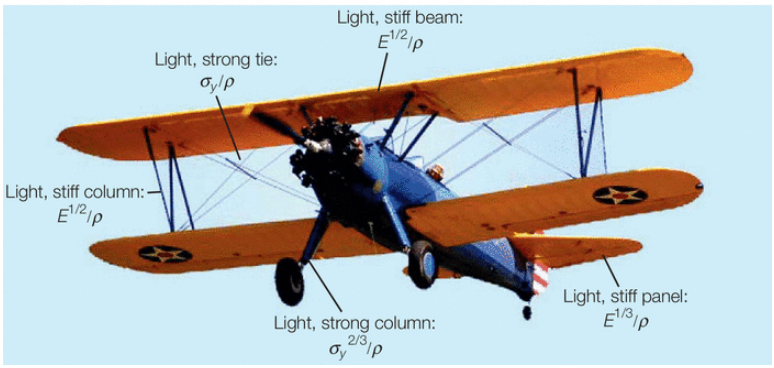

Figure 1: Example material indices for a biplane [1].

based optimization. Both approaches are employed to obtain the performance metric for the two-plate hot shock problem and are compared based on the results.

The rest of the report is structured as follows: Section 2 explains the proposed approaches in greater detail. Section 3 presents the traditional approach for determining the performance metric for the canonical beam bending problem. Section 4 presents the two-plate hot shock problem along with its associated complexities. Section 5 presents the results from the implementation of the two approaches on the two problems and Section 6 discusses the conclusions and potential future work as discerned from the project. References concluded the report.

2 Proposed Methods

The unsupervised feature selection based optimization approach consists of the following stages:

1. Find optimal values for material and geometry for different values of a certain material property (beam stiffness for the beam bending problem and frame safety factor for the hot shock problem) through multiple lookup table based optimization routines.
2. Optimize for the performance metric via regression (which is a function of the optimal set of properties from stage 1) to obtain the performance indices.
3. Perform the optimization routine in stage 2 inside a feature selection routine to identify the combination of free variables that minimizes the residual between materials.

The optimal features obtained in Stage 1 are merely interpreted to have the most influence on the resulting performance metric. This however means that the selection of optimal features will depend on the data used and must be kept in mind. Feature selection in the feature-selection-based optimization approach is conducted by using Sequential Forward Search and a normalized mean absolute error metric is used as the class separability criterion. The normalized mean absolute error is defined as:

$$\epsilon = \frac{1}{\bar{y}} \frac{\sum_{i=1}^{n} |y_i - \bar{y}|}{n}, \tag{1}$$

where y_i is the measured value of each datapoint, $\bar{y}$ is the mean value of all datapoints (operating on the hypothesis that if all y_i are identical, the optimal material index is found), and n is the number of datapoints. Normalization of the error metric is essential for this problem, as material indices may vary by many orders of magnitude; a typical mean absolute error would not capture this variation and instead converge to the lowest value of the material index.

The neural network-based feature selection and optimization approach involves the selection of the optimal set of features using a wrapper feature selection approach, which provides as a by-product the trained neural network for that feature set. It involves the following steps:

- Perform wrapper feature selection using the neural network with the class separability criterion as the adjusted R^2 metric.

- Use the resulting trained Neural Network as the evaluator for the Genetic Algorithm to solve the constrained optimization problem. Store the resulting optimal feature values.
- Optimize for the performance metric (which is a function of the optimal features from step 1) to obtain the performance indices.

Wrapper feature selection is carried out using Sequential Forward Search and the adjusted R^2 metric as computed using the appropriate neural network is used as the class separability criterion. For reference the adjusted R^2 metric is shown in Equation 2.

$$R^2_{adj} = 1 - \frac{RSS/(n-d-1)}{TSS/(n-1)} \tag{2}$$

RSS is the residual sum of squares computed as the loss function value for the neural network as computed on the training data, n is the total degrees of freedom, d is the number of features considered to create and train the neural network, TSS is the total sum of squares which is the RSS as computed assuming a zero dimensional surrogate model, i.e. the mean value of the response is assumed to be prediction of the surrogate model for all inputs. It is obvious that the TSS will always be higher than the RSS since the use of features is bound to improve the predictability of the resulting surrogate model. The adjusted R^2 metric quantitatively represents the balance between increased dimensionality of the neural network inputs and the improvement in its predictive capability and hence can be used to compare surrogate models of varying feature dimensionality.

The performance metric is of the form

$$P = x_1^{k_0} x_2^{k_1} ....x_m^{k_{m-1}}$$

where $[x_1, x_2, ..., x_m]$ are the features determined through feature selection and $[k_0, k_1, ..., k_{m-1}]$ are the performance indices determined through optimization.

It is important to note that the performance metric depends on the material property optimized in Stage 2. The optimization routine in Stage 3 endeavors to determine the set of performance indices for which P will be invariant through the optimal values obtained in Stage 2.

3 Example 1: Light, stiff beams

To demonstrate the feasibility of a machine-learned material index, a canonical problem is first used. In this example, the lightest beam with fixed length and square cross-section that can withstand a deflection δ is sought. As shown in this section, the material index for this type of problem is known to be $\sqrt{E}/\rho$. We show that our machine learning techniques can converge on the same solution.

3.1 Dataset creation

The beam dataset consists of 65 different engineering materials, including metals, ceramics, natural materials and polymers. For each candidate material, three features are recorded: Young's Modulus, density, and the category to which each material belongs (e.g., Non-ferrous metals). The dataset was compiled from *Materials Selection in Mechanical Design* [1]. A plot of the dataset plotted in log-log space is shown in figure 2.

3.2 Determination of performance index via traditional methods

Ashby hypothesized that the performance of an engineering component can be written as a separable function of three groups of parameters:

$$P = f(F, G, M) = f_1(F) \times f_2(G) \times f_3(M), \tag{3}$$

where F describes the functional requirements (e.g., carry loads, transfer heat, etc.), G specifies the component geometry, and M includes the material properties. To maximize performance, one must maximize the functions that depend of the *free variables* of the specific problem to be solved, which are most commonly functions of solely material properties. The strategy by which one formulates the performance metric is detailed below for a stiffness-constrained square beam in bending of minimum mass.

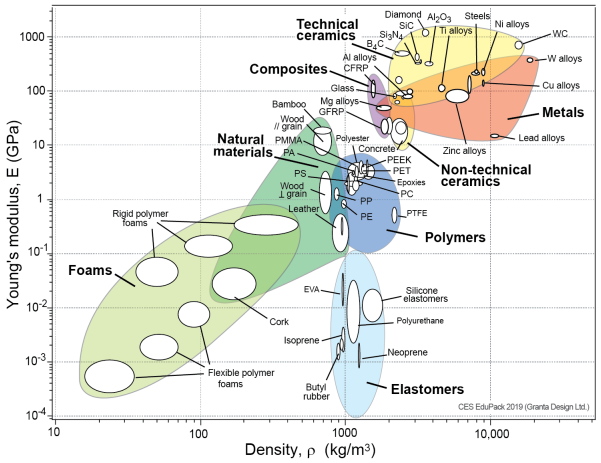

Figure 2: Ashby plot of the dataset used in the beam example.

1. State the objective function. As mass is the objective to minimize:

$$m = \rho A l, \tag{4}$$

where ρ, A, and l denote the material density, cross-sectional area, and length of the beam, respectively.

2. Formulate the constraint. In this example, the beam is stiffness-limited. Thus, the constraint can be written as:

$$\text{Stiffness} = K = \frac{F}{\delta} \geq \frac{CEI}{l^3}, \tag{5}$$

where F is the applied force and δ is the resulting displacement. This can be written strictly in terms of material and geometric properties, namely C (a constant value of 3), E (material Young's modulus), I (beam moment of inertia), and l.

3. Solve for the fixed variables in the constraint. As the beam is specified to be a constant square cross-section, A is the fixed variable that appears in the objective function (by manipulation of the moment of inertia).

$$K \geq \frac{CEA^2}{12l^3} \rightarrow A \leq \sqrt{\frac{12Kl^3}{CE}} \tag{6}$$

4. Substitute the expression for the fixed variables into the objective function.

$$m \geq \left(\frac{12Kl^3}{C}\right)^{1/2} (l) \left(\frac{\rho}{\sqrt{E}}\right) \tag{7}$$

This function now can be described as a separable function, where the free variables specific to material properties are grouped together. From this analysis, it is shown that the optimal material to minimize mass in a stiffness-constrained beam are those with a minimum value of $\rho/\sqrt{E}$.

The above procedure has been validated for a wide range of different use cases, from radome materials that minimize distortion to structural components that maximize energy absorption. However, when the functions that describe performance are not analytically tractable and require solution via numerics, novel methods such as those presented herein are essential.

4 Example 2: Hot shock considering dissimilar materials

As an extension of machine-learned material indices to a more complex problem in which the solution cannot be analytically determined, a two-material assembly undergoing hot shock is considered.

Hot shock is associated with engineering applications in which a component rapidly experiences an increase in environmental temperature, and large tensile stresses form at the component midplane [2]. While material indices exist for cases in which the components can be assumed to be infinite, in many instances the interactions between materials dominate failure modes. Complicating this problem further are size effects that are a function of the component geometry. This class of problem requires novel methods to perform material selection to downselect efficiently, as well as highlight what material properties (or combinations thereof) need to be targeted for future research and development.

4.1 Materials dataset

As this problem has multiple conflicting requirements and the interactions between frame and pane materials may produce non-intuitive results, even preliminary material selection is no trivial matter. To survive the harsh thermal environment associated with the specific hot shock scenario we are analyzing, only ceramic matrix composites are considered herein. The preliminary materials dataset consists of 13 materials: 10 pane materials and 3 frame materials. Figure 3 depicts these candidate materials contextualized in material index space (considering a infinite homogeneous body), where frame materials are shown in greyscale and pane materials are shown in shades of blue and green. Figure 3a compares the time before material failure with the material thermal strain, figure 3b compares strength-controlled (proportional to failure strength) and toughness-controlled (proportional to fracture toughness) thermal shock resistance. Following the design principles detailed in Ashby [1], optimal materials lie in the lower-right corner of figure 3a, as this will maximize the time to failure while minimizing the material thermal strain. It can be seen that from this analysis, Carbon/Silicon Carbide (C/SiC), Slip-Cast Fused Silica (SCFS), and Nextel 720 (Ox-Ox) appear to the best materials with respect to thermomechanical performance. However, that conclusion is complicated upon inspecting figure 3b. From the work of Lu and Fleck[2], to balance strength-controlled and toughness-controlled failure, a material must lie on the design guidelines shown, and furthermore, should ideally exhibit similar orders of magnitude of both material indices (i.e., an ideal material will have the same strength-controlled and toughness-controlled thermal shock resistance). While C/SiC appears to lie on the guideline, it can be seen that SFCS exhibits higher strength-controlled thermal shock resistance and may be susceptible to fracture. Finally, this entire analysis discounts the effects of geometry and material compatibility, which may dominate the design space.

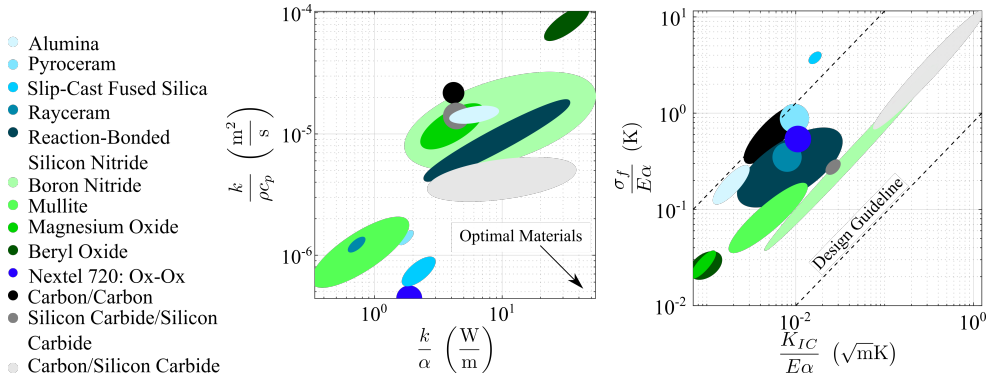

(a) Thermal diffusivity and thermal strain for candidate frame and pane materials.

(b) Strength-controlled and toughness-controlled thermal shock resistance for candidate frame and pane materials.

Figure 3: Relevant material indices for candidate frame and pane materials.

4.2 Structural analysis

In this work, we consider a regular hexagonal plate composed of two dissimilar ceramic materials. The pane (shown in light blue in figure 4a) is bounded on all sides by an integral frame (shown in black and gray). Additionally, the geometry of each hexagon is parameterized by four design variables: the hexagonal area (A), frame thickness (t), plate depth (d), and fillet radius (r). The hexagonal area controls the overall area of the plate, while the frame thickness denotes the portion of the plate that is comprised of frame material. The plate depth describes the distance that the plate is

extruded in the z-direction, and the fillet radius describes the radius of curvature of each of the frame fillets.

To analyze the hexagonal plate as if it were embedded in a larger structure undergoing hot shock, the following boundary conditions were applied. An encastre (all degrees of freedom fixed) boundary condition is specified on the inside edge of the plate (x=y=max, z=0). To allow for expansion, the side faces (e.g., the faces in which the normal direction is perpendicular to the z-direction) are fixed in x and y, but free to expand in the z-direction. A transient heat flux of 101 x $10^3 \mathrm{W/m^2}$, which corresponds to the aerodynamic heating flux associated with a Mach 5 stagnation point at 20 km of altitude, was applied to the exterior face (z=d) of the plate. Additionally, a radiative cooling flux was applied to the exterior face, where the total emissivity was assumed to be 1 and the external sink temperature was approximated to be -56°C. On the interior face (z=0), free convection and radiative cooling to a sink temperature of 20°C was applied to simulate the heat rejected to the vehicle interior.

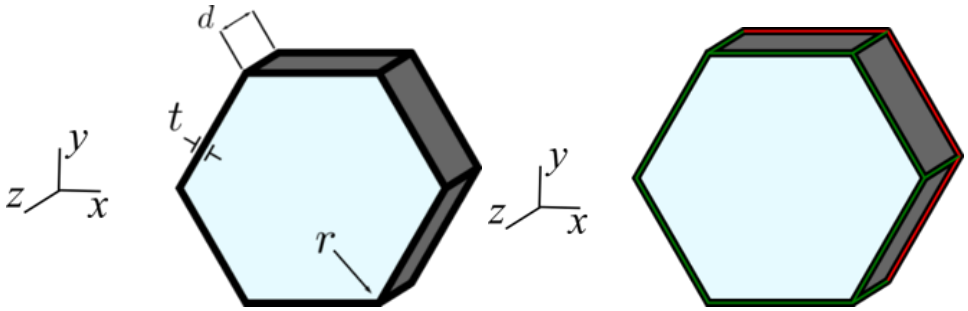

(a) Notional geometry and design variables. (b) Structural boundary conditions.

Figure 4: Geometrical description of the design space.

Finite element analysis considering transient heat transfer and nonlinear geometric effects was completed in Abaqus for each design. A full-factorial design of experiments over all possible pane and frame material combinations and geometric design variables was conducted, resulting in upwards of 500 data points. For each design, safety factors of both the frame and pane materials were calculated based on the maximum Von Mises stress attained:

$$\mathrm{SF} = \frac{\sigma_{\mathrm{yield}}}{\sigma_{\mathrm{max}}} \cdot |_{\mathrm{pane,frame}} \tag{8}$$

Additionally, a first-order approximation of structural fracture toughness was conducted by assuming a mode I crack embedded at the midplane of each material, where the crack is of length 1.0 mm (denoted by a). Fracture stress is calculated according to the following expression:

$$\sigma_{\mathrm{fracture}} = \frac{K_{IC}}{\sqrt{\pi a}}, \tag{9}$$

and a fracture toughness factor is determined by normalizing each fracture stress by the maximum tensile strength of each material considered:

$$\mathrm{FF} = \frac{\sigma_{\mathrm{fracture}}}{\sigma_{\mathrm{max,tensile}}} |_{\mathrm{pane,frame}} \cdot \tag{10}$$

For each analysis, four scalar performance metrics are determined and can be seen in figure 5. The red shaded area in each plot denotes the regions in which a material fails during analysis, and each plot is color-coded according to the frame and pane materials of each design. It can be seen that while the material indices may predict some performance (e.g., the best strength-controlled thermal shock resistance designs include SCFS panes), applying that logic ubiquitously is misleading and a gross oversimplification. In this work, we aim to determine optimal material indices for strength- and toughness-controlled thermal shock resistance that include the interaction between materials as well as geometric effects.

To obtain the most compact representation of the performance metric in terms of the material and geometric properties, feature selection is used to determine the optimal set of features.

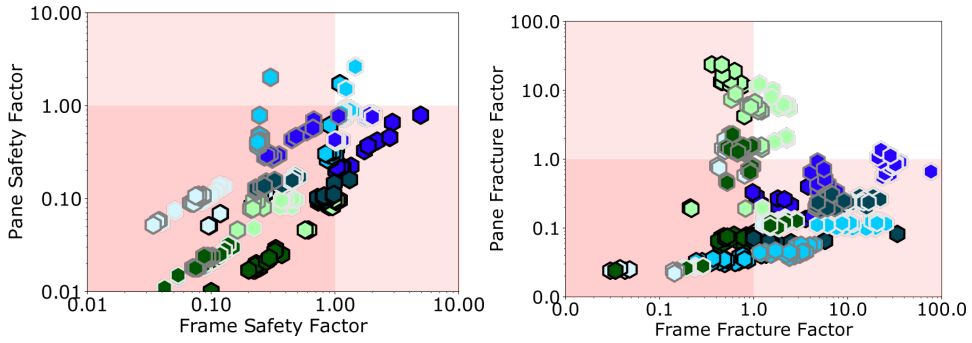

(a) Strength-controlled thermal shock resilience. (b) Toughness-controlled thermal shock resilience.

Figure 5: The strength and toughness controlled thermal shock resilience plots are shown. For each datapoint, the border color represents a material choice for the pane and the infill color represents a material choice for the frame.

5 Implementation Results

The results from the implementation of the two proposed approaches to the two problems are presented below. The unsupervised feature selection based optimization approach is implemented on both the beam bending and two plate hot shock problems whereas the neural network based feature selection and optimization approach is implemented on the two plate hot shock problem only, due to the triviality of the beam bending problem.

5.1 Unsupervised Feature-Selection based Optimization

As a brief review, the unsupervised feature selection-based optimization method consists of three main stages: compilation of an optimal set given a engineering problem, performance metric optimization to find a common material index across the optimal set, and feature selection to identify the optimal features (if necessary).

5.1.1 Beam Bending

In the beam bending example, the optimal set was found by solving the following optimization problem:

$$\min_{\text{material}} \; m = \rho A l \tag{11}$$

$$\text{s.t. } K \geq \frac{CEI}{l^3} \tag{12}$$

for a range of different constraint values K. The results of the first-stage optimization are displayed in table 1. Upon inspection, all members of the optimal set agree with intuition, as they are all materials with which beams under bending may be constructed, subject to a stiffness constraint. The one outlier may be Silicon, as in practice Silicon is very expensive and brittle, but that level of fidelity was not captured in the optimization (e.g., fracture toughness or cost per unit mass were not features).

Table 1: Optimal set for the beam under bending.

Material	E (GPa)	ρ (Mg/m^3)
Rigid polymer foam	0.051	0.05
Wood (longitudinal)	13	0.7
Carbon Fiber-Reinforced Plastic (CFRP)	109	1.55
Silicon	147.5	2.32

Optimization to find a common performance metric via regression was conducted by minimizing the error between each performance metric given a set of powers with which to operate on the features

(in this case, E and ρ). In this stage, the set of powers are the design variables, and are constrained to be between -3 and 3, in addition to being either integer or integer fractions. This constraint was defined to force the optimizer to converge to values that were comparable to work in literature, even though for more complex problems there is no guarantee for round powers. The sensitivity of the material index to this constraint may be investigated in future work.

$$\min_{x_1,x_2} \epsilon = ||\mathbf{P}^{\text{material}}|| \tag{13}$$

$$\text{where } P_i = E_i^{x_1} \rho_i^{x_2}, \tag{14}$$

$$x_i \in [0, \pm\frac{1}{3}, \pm\frac{1}{2}, \pm 1, \pm 2, \pm 3] \tag{15}$$

The performance metric optimization was implemented by using a 50-member, 50-generation genetic algorithm from the python package DEAP[2]. The converged solution was found to be

$$P = E^{-1}\rho^2 = \frac{\rho^2}{E}, \tag{16}$$

which can be shown to be functionally equivalent to the known optimal material index for this problem ($\rho/\sqrt{E}$). This result shows that this method may have utility to find material indices, but is very sensitive to the dataset from which the optimal set is derived. If the materials dataset used for this problem included more novel materials that occupy a high-stiffness, low-density regime (such as architected composites), the optimal set would be drastically different and thus the material index may be incorrect.

5.1.2 Hot Shock considering Dissimilar Materials

For the hot shock example, the optimal set was found by optimizing the frame fracture factor with a constraint on the pane fracture factor (represented graphically as the pareto-optimal set in the bottom-right corner of figure 5b). This optimal set is displayed in table 2, with constituent frame and pane materials shown as well.

Table 2: Optimal set for the hot shock problem.

Fracture Factor	Frame Material	Pane Material
0.06	C-SiC	MgO
0.15	SiC-SiC	Alumina
2.22	SiC-SiC	SCFS
3.95	SiC-SiC	SCFS
5.74	C-C	RBSN
25.55	C-SiC	SCFS
76.71	C-SiC	Ox-Ox

This problem considered many more features than the beam example, so Sequential Forward Search was implemented. The features considered are the following:

- Material Properties: Young's Modulus E (in GPa), coefficient of thermal expansion α (in 10^{-6}/K), fracture toughness K_{IC} (in MPa $m^{1/2}$), thermal conductivity k (in W/m-K) and thermal diffusivity κ (in Wm^2/J) for both frame and pane.
- Geometrical Properties: Pane Area A (in m^2), frame thickness t (in m), plate depth d (in m) and fillet radius r (in m).

For each combination of potential features, as genetic algorithm was implemented to find the optimal performance index:

$$\min_{x_1,x_2,\ldots,n} \epsilon = ||\mathbf{P}^{\text{material}}|| \tag{17}$$

$$\text{where } P_i = F_i^{(1)x_1} F_i^{(2)x_2} \ldots F_i^{(n)x_n}, \tag{18}$$

$$x_i \in [0, \pm\frac{1}{3}, \pm\frac{1}{2}, \pm 1, \pm 2, \pm 3] \tag{19}$$

[2]For brevity, the full optimization parameters are not detailed here, but can be made available upon request.

where once again the error metric was defined to be a normalized mean absolute error.

Sequential Forward Search was conducted for 2 to 7 features, and the results of this analysis are shown in table 3. From the results, it appears that the optimal material indices are only predicted by including the frame Young's Modulus and the frame thickness, and adding additional features does not decrease the mean absolute error. In fact, as is the case with 6 and 7 features, adding additional features increases the mean absolute error, which may indicate overfitting the data. However, these conclusions are further complicated when inspecting the optimal powers for the material indices. As $x_i = 0$ is a possible power (which would result in that feature not having any influence on the material index), this inclusion acts as a second form of feature selection. In fact, all feature sets that have less than 6 features have converged to values in which most features are eliminated during optimization (e.g., $I = E_{frame}^{0} t_{frame}^{0.33}$). For this reason, it seems as though either the guiding hypothesis for this work (there exists a common optimal material index for the optimal set), or the methods are flawed. To remedy this problem, the optimal set could be comprised of more points, or the material index optimization could be changed to not consider powers of zero. Alternatively, feature selection could be conducted in an "inverse" manner, where the designer simply specifies how many features may converge to a power of zero. This method will be investigated in future work.

Feature Set	Normalized MAE
$[E_{frame}$ frame thickness$]$	0.004
$[E_{frame}$ frame thickness $K_{IC,frame}]$	0.004
$[E_{frame}$ frame thickness $K_{IC,frame}$ $E_{pane}]$	0.004
$[E_{frame}$ frame thickness $K_{IC,frame}$ E_{pane} $k_{pane}]$	0.004
$[E_{frame}$ frame thickness $K_{IC,frame}$ E_{pane} k_{pane} $\alpha_{pane}]$	0.013
$[E_{frame}$ frame thickness $K_{IC,frame}$ E_{pane} k_{pane} α_{pane} pane depth$]$	0.07

Table 3: The feature sets found using Sequential Forward Search are shown along with their normalized mean absolute error.

5.2 Neural Network based Feature Selection and Optimization

For reasons of time, only the neural network based wrapper feature selection process was conducted. However, the specific optimization problems to solved in steps 2 and 3 from the approach description in Section 2 are described below, along with the results from the feature selection process.

5.2.1 Hot Shock considering Dissimilar Materials

The features considered for this problem are the following:

- Material Properties: Young's Modulus E (in GPa), coefficient of thermal expansion α (in 10^{-6}/K), fracture toughness K_{IC} (in MPa $m^{1/2}$), thermal conductivity k (in W/m-K) and thermal diffusivity κ (in Wm^2/J) for both frame and pane.
- Geometrical Properties: Pane Area A (in m^2), frame thickness t (in m), plate depth d (in m) and fillet radius r (in m).

This makes a total of 14 features.

The neural network is a fully connected multilayer perceptron and has a simple structure described as follows:

- Input layer: size - $d \times 1$
- Hidden layer 1: input size - $d \times 1$, output size - 10×1, activation - RelU
- Hidden layer 2: input size - 10×1, output size - 5×1, activation - ReLU
- Output layer: input size - 5×1, output size - 2×1, no activation

The two outputs in this case are the frame safety factor and the pane safety factor. For each instance, the neural network is trained on the full dataset with batch size of 32 and for 20 epochs. The Adam[3] optimizer is used for training. The implementation of the neural network and its associated procedures is done using the tensorflow-Keras library in Python.

The results from Sequential Forward Search upto 8 features is shown in Table 4.

Feature Set	**Adjusted R^2 metric**
$[\alpha_{pane}]$	0.657507
$[\alpha_{pane} \quad k_{frame}]$	0.679383
$[\alpha_{pane} \quad k_{frame} \quad k_{pane}]$	0.594676
$[\alpha_{pane} \quad k_{frame} \quad k_{pane} \quad K_{IC,frame}]$	0.551149
$[\alpha_{pane} \quad k_{frame} \quad k_{pane} \quad K_{IC,frame} \quad \alpha_{frame}]$	0.605071
$[\alpha_{pane} \quad k_{frame} \quad k_{pane} \quad K_{IC,frame} \quad \alpha_{frame} \quad \kappa_{pane}]$	0.513795
$[\alpha_{pane}, k_{frame}, k_{pane}, K_{IC,frame}, \alpha_{frame}, \kappa_{pane}, d]$	0.412567
$[\alpha_{pane}, k_{frame}, k_{pane}, K_{IC,frame}, \alpha_{frame}, \kappa_{pane}, d, K_{IC,pane}]$	0.229478

Table 4: The feature sets found using Sequential Forward Search are shown along with their corresponding adjusted R^2 values.

From the table, it can be seen that the adjusted R^2 metric values are not very high for all the features found. This means that the neural network as described above is not able to reliably predict the safety factors. This may be due to two reasons. First, the neural network itself may be too simple and additional hyperparameter tuning is required to obtain the right architecture of the neural network. Second, the optimization process may have terminated prematurely, either due to local minima or not enough epochs being used. Additionally, more data could be used to improve the performace of the neural network.

From the set of features found, the best feature set is the set of $[\alpha_{pane} \quad k_{frame}]$. The reduction in the adjusted R^2 metric for subsequent features means that the addition of those features does not improve the predictability of the resulting neural network enough to justify the increased dimensionality. The sudden drop in the adjusted R^2 metric from the second last to last feature set is of special note. It is of note that all 10-dimensional feature sets result in negative adjusted R^2 values.

A key observation is that all feature vectors (except the last two) do not contain any geometric properties. This implies that the frame and pane safety factors are influenced more by the material properties than the geometric properties which is reasonable.

Note: During the implementation of the python script for this process, a bug was found wherein the neural network used only the first 11 datapoints for training instead of cycling through the complete dataset. This was identified as a known bug in the online forums and the resolution is to switch to a different nightly build of tensorflow. However, this was not done for this project.

Once the optimal feature set is identified, the next step is to solve the constrained optimization problem to determine the optimal datapoints with respect to a certain performance requirement. For the hot shock problem, the goal is find the performance metric for the datapoints with the highest frame safety factor for a certain value of pane safety factor. These points are the ones on the right side in Figure 5a. To determine these points multiple constrained optimization problems were proposed to be conducted to maximize frame safety factor for different ranges of the pane safety factor (represented as an inequality constraint). The domain of optimization was to be strictly the datapoints already present in the training dataset with the neural network outputs being used as the evaluation and constraint values. Although, the idea of using neural networks (or any other machine learning based surrogate model) is to be able to extend the optimization domain to datapoints outside of the training dataset. In that case, it would be advisable to use the adjusted R^2 metric computed using test error instead of resubstitution error as the class separability criterion for feature selection. For this project the Genetic Algorithm was proposed as the optimization algorithm since objective and constraint evaluation would be cheap.

The final step would be to determine the performance indices through optimization. This process would be similar to the one described in the unsupervised feature selection based optimization approach. But the key difference would be the features for which the performance indices are to be computed, which are computed using the neural network based adjusted R^2 metric as the class separability criterion in this approach.

6 Conclusions and Future Work

In this work, two novel methods for computing material indices were investigated: an unsupervised Feature-Selection based Optimization approach, and a Neural Network based Feature Selection and Optimization approach. Both methods have the potential to revolutionize materials selection for complex problems where analytical solutions are unattainable, giving designers greater flexibility in the type of problem than can be analyzed.

While the unsupervised Feature-Selection based Optimization approach was able to predict the correct material index for a simple stiffness-constrained beam in bending, it failed to predict a believable material index for the more complex hot shock problem. This failure may be due to a small dataset, errors in the guiding hypothesis, or errors in implementation. In future work, we will investigate different methods with which to conduct feature selection, as well as refine the optimization approaches both for finding the optimal material index and construct the optimal set.

The results from the neural network based feature selection and optimization approach and their explainability suggests that this approach does have scope for identifying the optimal material and geometric properties and their corresponding performance indices for complex material selection problems. The use of neural networks also brings the possibility of adding additional material and geometric datapoints for optimization. However, the relatively low adjusted R^2 metric values for the various feature sets does suggest that additional hyperparameter tuning must be performed for optimal operation. Since the neural networks would be used for optimization in the intermediate step, the high predictability of the neural network must be ensured so not to identify unwanted or incorrect datapoints as optimal.

In the future, the possibility of using other surrogate models like nonlinear Support Vector Machines or Gaussian Processes could be explored. The use of the latter opens the possibility of using other class separability criteria such as Bayesian Information Criterion (BIC). The use of Gaussian Processes would also naturally lead to the possibility of using Bayesian Optimization for the intermediate step instead of the Genetic Algorithm. Additionally, other optimization objectives for the determination of the performance indices could be used, for example the combinatorial sum of differences.

References

[1] M. F. Ashby, Materials Selection in Mechanical Design (4th Edition)Publisher: Elsevier.
URL https://app.knovel.com/hotlink/toc/id:kpMSMDE022/materials-selection-in-2/materials-selection-in-2

[2] T. Lu, N. Fleck, The thermal shock resistance of solids, Acta Materialia 46 (13) (1998) 4755–4768. doi:10.1016/S1359-6454(98)00127-X.
URL https://linkinghub.elsevier.com/retrieve/pii/S135964549800127X

[3] D. P. Kingma, J. Ba, Adam: A method for stochastic optimization, arXiv preprint arXiv:1412.6980 (2014).